Available online at www.sciencedirect.com

SCIENCE DIRECT®

Earth and Planetary Science Letters 229 (2005) 217–230

EPSL

www.elsevier.com/locate/epsl

Grain scale deformation in ultra-high-pressure metamorphic rocks—an indicator of rapid phase transformation

Annette Lenze[a], Bernhard Stöckhert[a,*], Richard Wirth[b]

[a]*Institut für Geologie, Mineralogie und Geophysik, Ruhr-Universität Bochum, Universitätsstraße 150, 44780 Bochum, Germany*
[b]*GeoForschungsZentrum, Telegrafenberg, 14473 Potsdam, Germany*

Received 4 February 2004; received in revised form 24 July 2004; accepted 13 October 2004

Editor: E. Boyle

Abstract

Conspicuous grain scale deformation is observed in some ultra-high-pressure (UHP) metamorphic rocks of the Dora Maira Massif, Western Alps, although no significant strain is discernible on the mesoscopic scale. In a jadeite–kyanite–quartz rock, some of the jadeite crystals reveal (100) deformation twins, indicating local differential stress levels above 0.3 GPa. Many kyanite crystals show marked kink or deformation bands, with a slip system (100)[001]. In contrast, the adjacent coarse-grained quartz matrix (grain size ca. 0.2 mm), which has formed from coesite during exhumation from >100 km depth, reveals a foam structure. The quartz grain boundary configuration is controlled by interfacial free energy, the grains are optically strain-free, and there is no crystallographic preferred orientation. Preservation of this foam microstructure, which indicates grain growth during low-stress annealing, precludes that deformation of the jadeite and kyanite crystals is a result of a late-stage low-temperature overprint. The orientation distribution of jadeite and kyanite with and without twins or deformation bands, respectively, has been investigated with a combination of universal stage and EBSD techniques. On the scale of a thin section, there is no preferred orientation of twinned jadeite and bent kyanite crystals and undeformed crystals, respectively. Thus, the orientation of the inferred local shortening direction is random. This precludes deformation driven by a homogeneous far field tectonic stress, but suggests an internally controlled stress field which is highly inhomogeneous on the scale of a few grain diameters. Laboratory experiments show that the coesite to quartz transformation proceeds within hours after decompression from 3.0 to 2.7 GPa at 800 °C. The microstructures of incompletely transformed samples indicate that the quartz growing at the expense of coesite undergoes crystal plastic deformation and recrystallizes with a very fine grain size during transformation. In this case, the deformation of quartz is attributed to the volumetric strain ΔV=+10% inherent in the coesite–quartz transformation, which causes a highly inhomogeneous stress field inside the sample related to the progress of the transformation. We propose that a similar process has taken place in the polyphase natural rock during exhumation, with the transient stresses causing mechanical twinning of jadeite and bending or kinking of kyanite. When the transformation had gone to completion, grain growth obliterated the microstructures of the quartz matrix, while the deformed jadeite and kyanite crystals

* Corresponding author. Tel.: +49 234 32 23227; fax: +49 234 32 14572.
E-mail addresses: annette.lenze@rub.de (A. Lenze), bernhard.stoeckhert@ruhr-uni-bochum.de (B. Stöckhert), wirth@gfz-potsdam.de (R. Wirth).

0012-821X/$ - see front matter
doi:10.1016/j.epsl.2004.10.012

preserved the record of inhomogeneous deformation at high temperatures. The peak differential stresses locally exceeded 0.3 GPa, which indicates very high strain rates and a correspondingly rapid transformation of coesite to quartz, comparable to the laboratory results.

Keywords: ultra-high pressure metamorphism; mechanical twinning; jadeite; kyanite; coesite–quartz transformation; volumetric strain

1. Introduction

The structures and microfabrics of exhumed ultra-high-pressure (UHP) metamorphic rocks can be used to provide important information on the conditions prevailing in subduction zones to depths of more than 100 km (e.g. [1]). Despite their rapid burial and exhumation (e.g. [2,3]) along a megascale shear zone, referred to as subduction channel, many of these rocks seem to have accumulated remarkably little strain during UHP metamorphism, as demonstrated by perfectly preserved magmatic fabrics of granites (e.g. [4,5]) and gabbros (e.g. [6]), or undistorted pillow structures in UHP metamorphic basalts (e.g. [7]).

The well-preserved UHP metamorphic rocks of the Brossasco–Isasca Unit of the Dora Maira Massif, western Alps, do not show evidence of notable deformation during or after UHP metamorphism. So far, strain shadows containing the UHP assemblage talc+phengite+kyanite at large pyrope crystals [8] are the only reported record of minor deformation at UHP metamorphic conditions. The UHP metamorphic Brossasco granite has retained undistorted magmatic structures, with coronitic structures discernible on the microscopic scale and fine-grained quartz aggregates [4,9]. The peculiar quartz microstructure is interpreted to indicate transformation of the original magmatic quartz to coesite, which was again replaced by quartz upon exhumation [4,10]. Wherever the granites of the Issasca Unit acquired a gneissic structure, the quartz microfabrics indicate deformation at greenschist facies conditions in a late stage of exhumation [11]. Altogether, the absence of notable deformation in the UHP metamorphic rocks suggests that the entire deformation during burial and exhumation was localised into weak shear zones, as proposed by Michard et al. [8], Stöckhert and Renner [12], and Stöckhert [1]. Mylonites unequivocally developed at UHP conditions have been rarely identified so far (e.g. [13,14]). While differential stress is proposed to be generally low during UHP metamorphism [1,12], peculiar microstructures including mechanical twins on the nanometer scale in omphacite and kyanite from a coesite eclogite have been interpreted to reflect a stage of high strain rate during exhumation and attributed to deep faulting by Hwang et al. [15].

In marked contrast to the obviously undistorted shape on the mesoscopic scale, some UHP metamorphic rocks of the Dora Maira Massif show mechanical twinning of jadeite, and conspicuous evidence of crystal plastic deformation of kyanite. This holds for the so-called pyrope quartzites with preserved coesite inclusions in garnet [16] as well as for adjacent jadeite–kyanite–quartz rocks. The presence of strain shadows with UHP mineral assemblages at pyrope [8] suggests deformation during UHP metamorphism by dissolution precipitation creep. This mechanism is activated at very low stress and hardly reconciles with crystal plastic deformation of jadeite and kyanite in these rocks, which is the objective of the present study.

In the following, we first examine the microstructures and orientation distribution of deformed and undeformed jadeite and kyanite crystals and the microstructure of the coarse-grained and almost strain-free quartz matrix, which must have formed from coesite during exhumation. We then report on microstructures of quartz developed in laboratory experiments upon transformation from coesite and, finally, discuss a possible scenario for the origin of the peculiar deformation features in the natural rocks based on a comparison with the experimental results.

2. Geological setting

The slices of UHP metamorphic continental crust in the southern Dora Maira Massif, western Alps, are described in much detail by, e.g. Chopin [16], Schertl et al. [17], Compagnoni et al. [18], Michard et al. [8], and Chopin and Schertl [19]. The UHP

metamorphic Brossasco–Isasca Unit (Fig. 1) mainly consists of fine-grained gneisses, which in places host lens-shaped bodies of various other rock types including metagranites, eclogites, marbles, and the conspicuous pyrope quartzites of whiteschist composition associated with jadeite–kyanite–quartz rocks (e.g. [16,17]). The characteristic mineral assemblages of the pyrope quartzites indicate peak pressures of up to 3.7 GPa at 700–800 °C (e.g. [16,17]). U–Pb data obtained on zircon and titanite using the SHRIMP microprobe [2,20] yield an age of about 35 Ma for the UHP metamorphism, and decompression to less than about 1 and 0.5 GPa by 32.9±0.9 and 31.8±0.5 Ma, respectively [2]. Cooling to below the closure temperature of fission tracks in zircon happened at 29.9±1.4 Ma [20], indicating that the rocks reached a position in the upper crust within ca. 5 million years after UHP metamorphism. This implies a rate of exhumation comparable to plate velocity [2]. Based on their age data, Rubatto and Hermann [2] propose a rate of about 3.4 cm/year for the earliest stage of exhumation, of 1.6 cm/year for the second stage, and of 0.5 cm/year for the latest stage, as visualized by the schematic pressure–temperature–time path shown in Fig. 2. According to the inferred pressure–temperature paths [17,19], the stability field of quartz was entered at temperatures of about 700–800 °C.

3. Sample description

Two representative samples (AL101, AL141) were chosen for the present study. They emanate from the

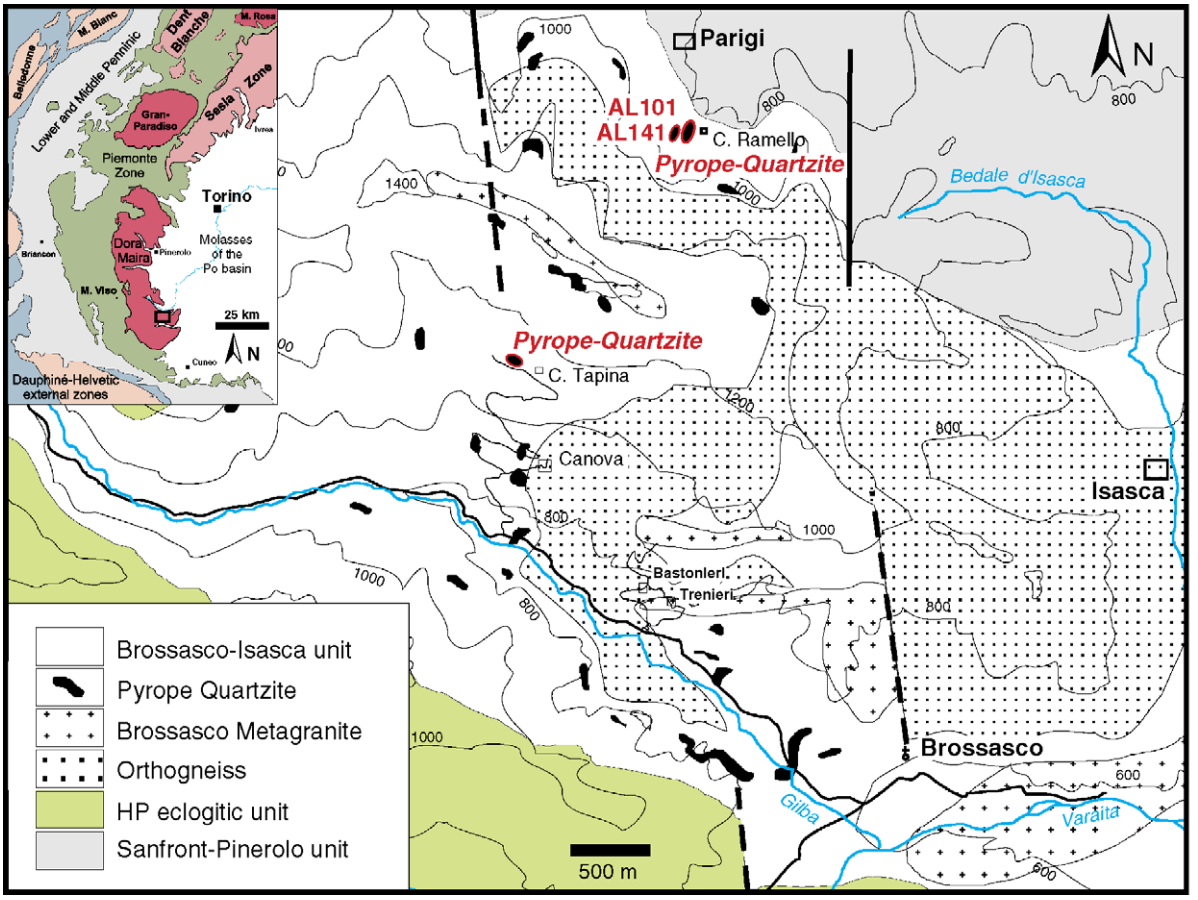

Fig. 1. Geological sketch map showing the southern Dora Maira massif after Henry [50] and Simon et al. [51], the Brossasco–Isasca Unit, and the sample locations.

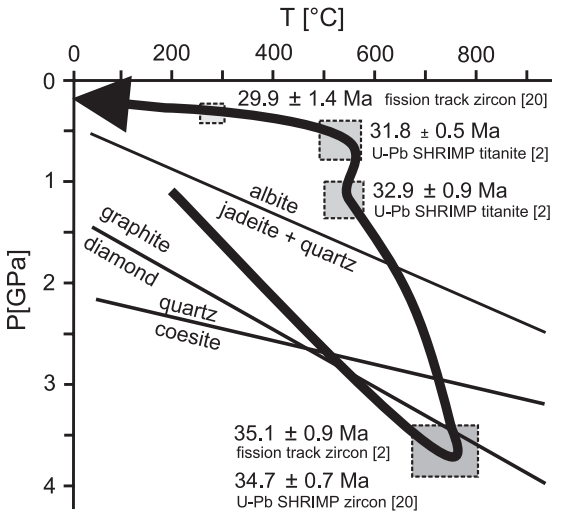

Fig. 2. *P–T* path of the ultra-high-pressure metamorphic rocks in the southern Dora Maira massif after Schertl et al. [17], with age constraints according to Gebauer et al. [21] and Rubatto and Hermann [2].

pyrope quartzite and the interlayered jadeite–kyanite–quartz rock from the outcrop at Parigi near Martiniana Po (e.g. [17]). Although the same deformation microstructures in jadeite and kyanite were observed in nearly identical pyrope quartzites and jadeite–kyanite–quartz rocks from the location Case Tapina [18], samples from that location have not been investigated further as the late transformation of jadeite to albite is almost gone to completion there.

The original UHP metamorphic mineral assemblage of the pyrope quartzite comprises coesite (now transformed to quartz, apart from relics preserved as inclusions in other UHP minerals), kyanite, garnet, phengite and, in places, jadeite, with accessory talc, apatite, zircon, pyrite and rutile [17]. The dark green jadeite-rich layer of both samples, with a thickness of ca. 5 cm, is made up by about 30% of jadeite and more than 50% of quartz, with minor kyanite, pyrope and phengite. In many places, the jadeite is rimmed by fibrous albite (Fig. 3a) with a composition of $Ab_{96}An_{3.5}Or_{0.5}$ [17]. In some domains, the reaction between jadeite and adjacent quartz has gone to completion, with no jadeite remaining. The grain size of quartz is between about 0.1 and 0.4 mm, and that of the other main constituents typically up to several millimeters.

The jadeite crystals are predominantly anisometric with a typical aspect ratio of ca. 1.5. In some areas, a weak shape preferred orientation of jadeite defines a foliation parallel to the compositional layering. The orientation of (100) and [001] of jadeite determined by universal stage and EBSD reveals no marked crystallographic preferred orientation (CPO) in sample AL141 (Fig. 4a) and a weak CPO in sample AL101 (Fig. 4b). Both compositional layering and weak preferred orientation are supposed to be inherited from a preexisting paragonite-bearing micaschist, the assemblage jadeite and kyanite representing

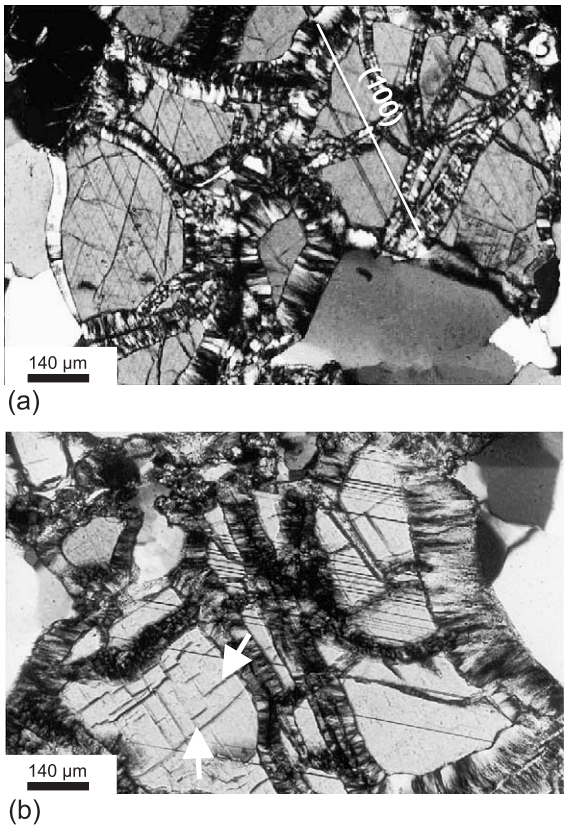

Fig. 3. (a) Optical micrograph of a jadeite crystal with mechanical (100) twin lamellae in sample AL101 (crossed polarizers). The trace of (100) is indicated. The jadeite is partially transformed into fibrous albite along former phase boundaries and cracks. (b) Optical micrograph of a jadeite crystal with thin (100) twin lamellae bisecting the {110} and {1$\bar{1}$0} cleavage (crossed polarizers). Some of the lamellae reveal a wedge shape and terminate within the crystal (arrows).

the high-pressure breakdown product of paragonite [17].

About 30% of all jadeite crystals embedded in quartz show lamellar mechanical twins of the (100)[001] type. They either maintain a constant thickness across the grains, or are wedge-shaped and terminate within the crystals (Fig. 3b). The twin density varies between 1 and 50 mm^{-1}, with a lamella thickness of <1 μm. No mechanical twins were found in jadeite crystals enclosed in garnet.

About 80% of the kyanite crystals embedded in quartz are bent or kinked. Kyanite inclusions in garnet crystals lack any evidence of deformation.

The quartz matrix hosting the deformed jadeite and kyanite crystals is characterized by predominantly isometric grains with plane or simply curved grain boundaries, which are optically strain-free. Undulatory extinction, subgrains and sutured high angle grain boundaries of quartz are restricted to sites where the adjacent jadeite crystals are largely or completely transformed to albite (Fig. 5a,b). These microstructural features are interpreted to reflect local deformation related to the volume change inherent in the late-stage transformation of jadeite+quartz to albite, superimposed on the previously developed foam structure.

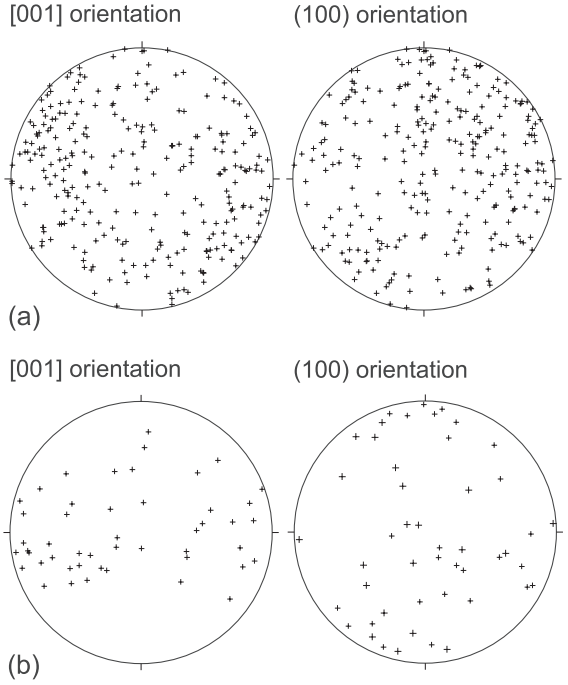

Fig. 4. (a) Stereographic projection showing the orientation of poles to (100)-plane and the [001]-directions of jadeite. There is no well-defined crystallographic preferred orientation in sample AL141. (b) In sample AL101, a weak crystallographic preferred orientation is evident related to the weak shape preferred orientation.

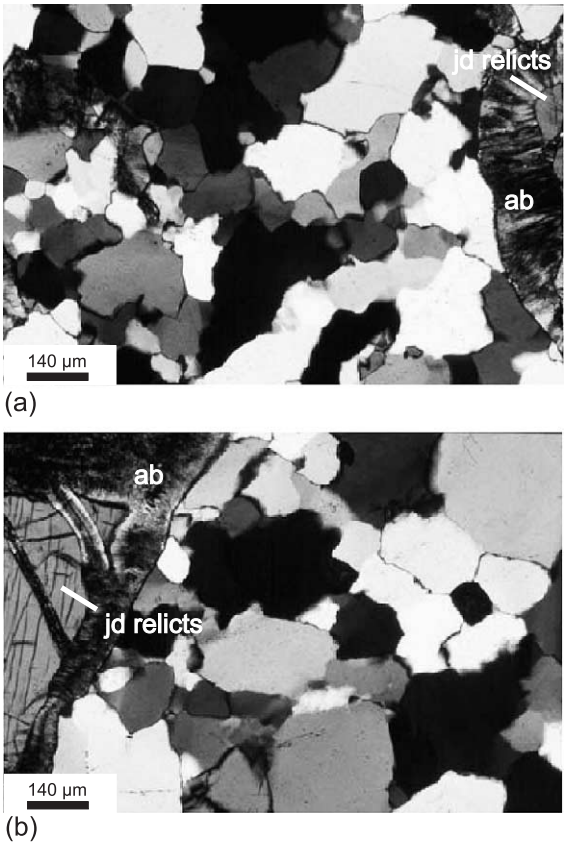

Fig. 5. Optical micrographs of quartz crystals adjacent to secondary fibrous albite rimming jadeite in sample AL101. In contrast to the foam structure predominantly developed elsewhere in the pyrope quartzites, at these sites a more irregular quartz microstructure is observed, with slightly sutured grain boundaries and weak undulatory extinction (crossed polars).

4. Methods

The samples were cut normal to the compositional layering and the foliation defined by the shape preferred orientation of phengite. A lineation is not obvious in the samples. From each sample, a set of both polished and glass covered thin sections were prepared. The mechanically polished thin sections

were additionally polished chemically using a silicon suspension (SYTON®).

The orientation of crystals and fabric elements was determined by a combination of polarizing microscopy with universal stage (Leitz Orthoplan), using the covered thin sections, and scanning electron microscopy (SEM) with electron backscatter diffraction facilities (EBSD), using the polished thin sections coated with carbon. The SEM used was a LEO 1530 with field emission gun and forescatter detector. Operating conditions for EBSD analysis were an accelerating voltage of 25 kV, with the section tilted over 70° and a working distance of 25 mm. The EBSD patterns were identified and evaluated with the software CHANNEL [21]. The orientations of the crystals are displayed with the program StereoNett [22].

5. Mechanical twinning of jadeite

Mechanical twinning of clinopyroxenes was studied by Raleigh and Talbot [23], Kirby and Christie [24], and Kollé and Blacic [25]. The critical shear stress for (100)[001] twinning of jadeite was determined as 150±25 MPa by Orzol et al. [26]. The presence of mechanical twins in jadeite crystals thus indicates that locally a differential stress of >300±50 MPa was achieved at a certain stage. On the scale of a thin section, the orientation distribution of jadeite crystals with and without twins can then be used to derive both a paleostress magnitude and the related orientation of the principal stress axes, as described by Trepmann and Stöckhert [27].

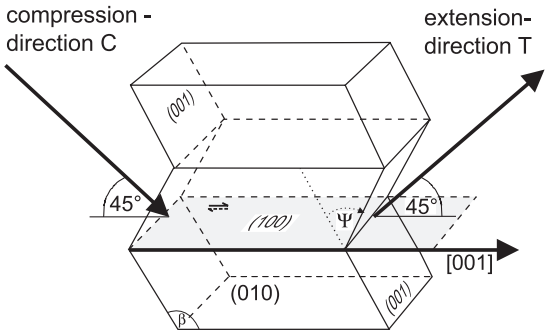

Fig. 6. Sketch showing the C- and T-directions for twinned jadeite as defined by Carter and Raleigh [52].

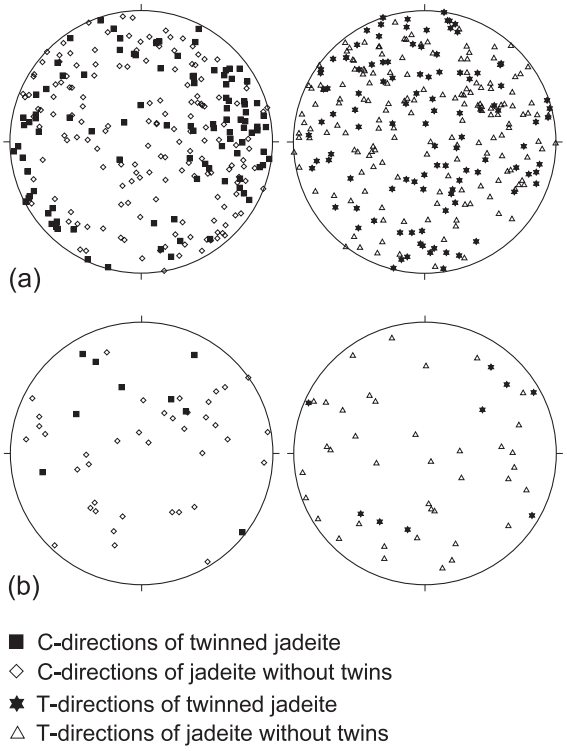

Fig. 7. (a) Stereographic projection showing the orientation of the C- and T-directions for 286 jadeite crystals with or without twins (differentiated by labels) in sample AL141. (b) The same for 48 jadeite crystals in sample AL101. There is no preferred orientation of crystals with or without twins.

As discussed by Raleigh and Talbot [23], the differential stress allowing twinning of jadeite is minimum if the major principal stress direction σ_1 parallels the compression axis C, which is oriented at 45° to (100) and [001] next to the optical axis X in the (010) plane, and the minor principal stress direction σ_3 parallels the tension axis T normal to C near Z in (010) (Fig. 6). Any orientation differing from this favourable one requires a higher differential stress for twinning.

In sample AL141, the crystallographic orientation of 268 jadeite crystals with and without mechanical twins has been determined in three thin sections, and that of 48 jadeite crystals in two thin sections of sample AL101. For each crystal, the C- and T-directions are constructed and displayed in stereographic projections (Fig. 7a,b), with the presence and absence of lamellar twins indicated by the labels. Fig. 7a and b shows that the orientation distribution of the

C- and *T*-directions of jadeite crystals with and without twins is random on the scale of a thin section for both samples.

6. Kink bands in kyanite

Kink bands in single crystals can be described as a pair of kink band boundaries (KBB), across which there is a change in orientation of the active slip plane (e.g. [28,29]). The change in orientation within one kink band, described as a rotation about the kink axis, is caused by translation on the active slip plane within the kink band, while the crystal beyond the kink band remains largely undeformed [30].

Kink bands develop in materials of high mechanical anisotropy upon shortening parallel or subparallel to a prominent glide plane (e.g. [31,30]). Their geometry was investigated in laboratory experiments on foliated rocks (e.g. [32]). When the maximum principal stress direction σ_1 was parallel or at a very low angle (α=0–5°) to the active slip plane, the formation of conjugate kink bands was observed. Single sets of kink bands were observed to develop at angles α between a few degrees and up to about 30°. The tendency to form kink bands was found to diminish when the angle α between the glide plane and the maximum principal stress direction σ_1 approached about 15–30°, with bend-gliding [31] along the slip plane becoming more effective. The KBB are found to develop at an angle of 45–60° to the maximum principal stress direction σ_1, independent on confining pressure and total strain [33]. Kink bands can be used to infer the principal stress directions [30].

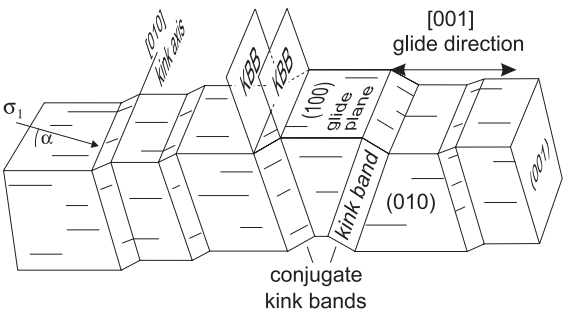

Fig. 8. Geometry of kink bands in kyanite, developed by (100)[001] glide.

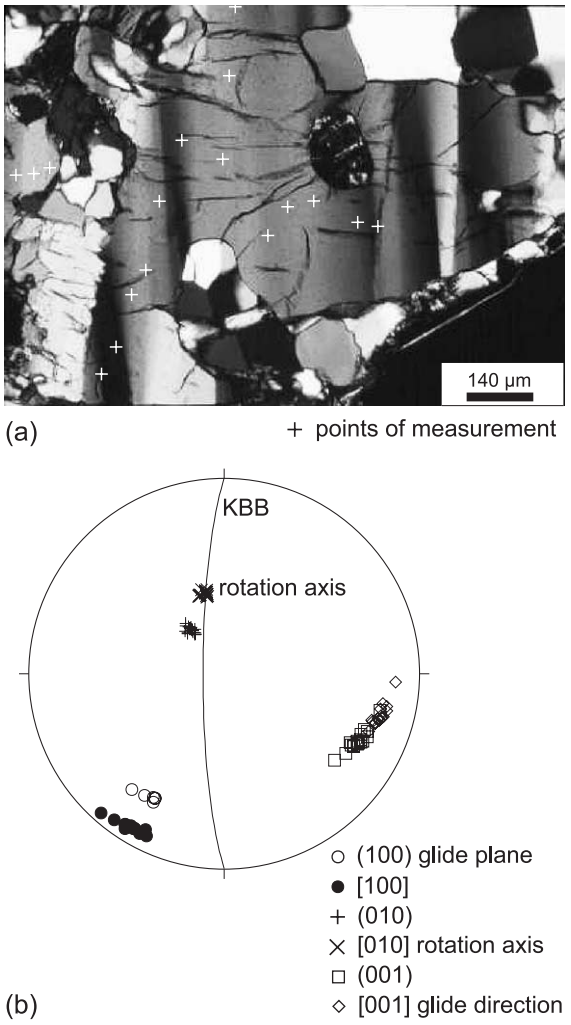

Fig. 9. (a) Optical micrograph showing kink band boundaries (KBB) in kyanite (crossed polarizers). (b) Crystal orientation determined by EBSD at different locations in a kinked kyanite crystal. The uniform orientation of [010] indicates a rotation about this axis. The geometry confirms the predicted glide system (100)[001].

The geometry of kink bands in experimentally deformed kyanite was investigated by Raleigh [34]. His deformation experiments were carried out at a confining pressure of 0.5–0.7 GPa and a temperature of 700–850 °C, with a sample strain of about 5–10%. The geometry of the kink bands indicates a glide plane (100) and a glide direction [001] (Fig. 8). The kink axis is oriented normal to the glide direction. Although conjugate kink bands with opposite sense of

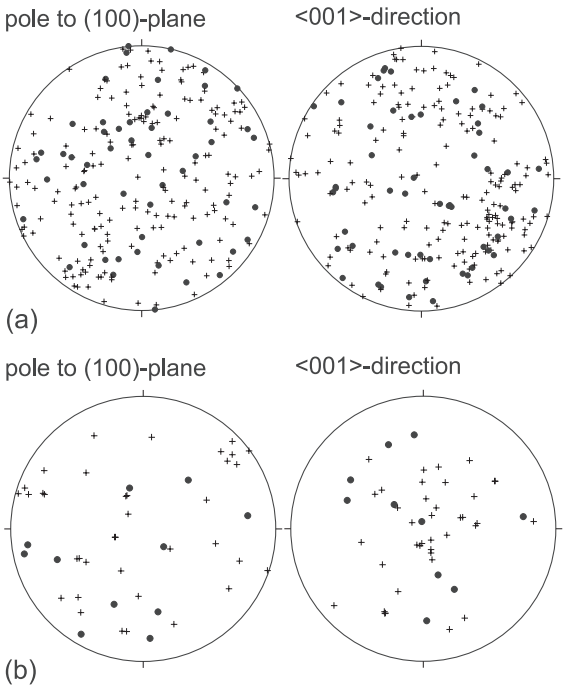

Fig. 10. Stereographic projection of the orientation of the glide plane (100) and the glide direction [001] of deformed (cross) and undeformed (black dot) kyanite crystals (a) in sample AL141 and (b) sample AL101. There is no preferred orientation of kinked or bent crystals.

shear were observed, their intersection has not been described so far in kyanite.

To confirm the predicted kink geometry in kyanite (Fig. 9a), the crystallographic orientation within kink bands and host crystals was determined. The stereographic projection (Fig. 9b) shows that the [010] direction is nearly identical for both sites and therefore represents the axis of rotation, referred to as the kink axis. The KBBs, visible in orientation contrast images obtained by SEM or in the polarizing microscope (Fig. 9a), contain the kink axis and are at a high angle to [001], which is the inferred glide direction. The kink axis and the glide direction define the glide plane (100). This geometry is consistent with the findings of Raleigh [34].

In the jadeite–kyanite–quartz rocks, the kyanite crystals show no lattice preferred orientation. The crystallographic orientation of 48 and 240 kyanite crystals with and without kink bands was determined in samples AL101 and AL141, using two and three mutually perpendicular thin sections, respectively. The glide direction [001] and the normal to the glide plane (100) of all kyanite crystals with and without kink bands are displayed in the stereographic projection in Fig. 10a and b. The diagrams reveal no preferred orientation of deformed or undeformed kyanite crystals.

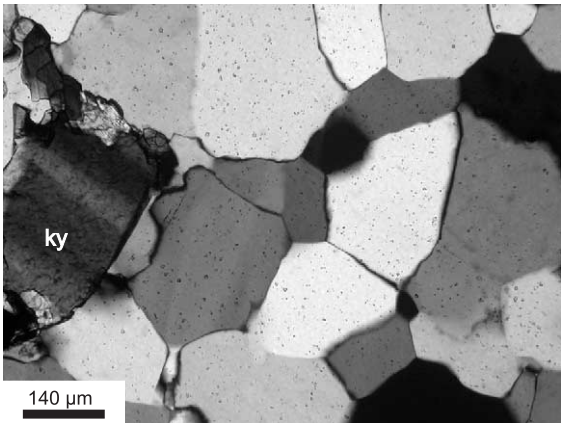

(a)

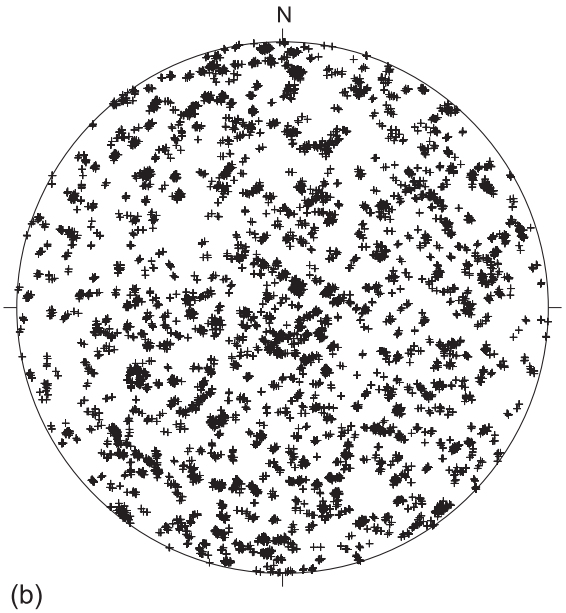

(b)

Fig. 11. (a) Optical micrographs showing the typical foam structure of the quartz matrix (crossed polarizers), and (b) stereographic projection of the orientation of (5396) quartz *c*-axes measured by EBSD over an area of ca. 3×3 mm in a quartz domain of sample AL141. There is no crystallographic preferred orientation of quartz.

7. Quartz microstructures

The microstructure of quartz surrounding the deformed jadeite and kyanite crystals is characterized by mostly isometric grains with plane or simply curved high-angle grain boundaries meeting at near to 120° angles at the grain edges (Fig. 11a). The microstructure is referred to as a foam structure. Most grains are optically strain-free, or very nearly so. The grain size is about 0.2 mm. The orientation of the quartz *c*-axes was determined in sample AL141 by automatic EBSD measurements over an area of ca. 3×3 mm with a step distance of 30 μm and a total of 5396 points. Fig. 11b shows that there is no CPO.

In places, the quartz grains are elongate and form a coarse palisade structure normal to interfaces with UHP mineral phases (e.g. [35]; Fig. 4). It is not clear whether this coarse palisade microstructure has a similar origin as the very fine-grained palisade structure developed where quartz replaces coesite in inclusions [16,36,37]. Apart from the elongate grain shape, the simple configuration of the high angle grain boundaries corresponds to that observed in the quartz aggregates with an isometric grain shape and a foam structure.

8. Microstructures of quartz grown at the expense of polycrystalline coesite in laboratory experiments

8.1. Experimental procedures

Synthesis of polycrystalline coesite and transformation experiments to quartz were carried out in a conventional solid medium piston cylinder apparatus with NaCl as the confining medium [38]. Silica glass (HERALUX, trademark) of high purity was used as starting material for the synthesis [39]. The glass was ground in an agate mortar and the grain size fraction <63 μm was separated by sieving. This powder was filled into gold tubes with an inner diameter of 3 mm, and then compacted under vacuum with an applied pressure of up to about 30 MPa. Adsorbed moisture was not removed prior to compaction. After compaction, the capsules were mechanically sealed by a gold coverplate.

Two samples were synthesized simultaneously at 3 GPa confining pressure and at a temperature of 800 °C, with a run duration of 60–111 h. One sample was used as a reference and inspected with respect to grain size, grain shape, and preferred orientation. When the reference sample showed a satisfactory homogeneous coesite microstructure, the twin samples were used for transformation experiments. Several small slabs were taken from one of the synthesized samples.

As the concentration of water-related defects in coesite is reported to affect the rate of transformation to quartz [36,40], the hydrogene content of the synthetic coesite was determined by FTIR microspectrometry on selected large single crystals with a thickness of 0.1–0.25 mm. The diameter of the analyzed spot was 0.08 mm. The large synthetic coesite single crystals contain between 100 and 600 H/10^6 Si.

For a transformation experiment, the selected synthetic coesite sample was remounted in a gold capsule and inserted in the piston cylinder apparatus, as described above. First, the pressure was built up to 3 GPa. Subsequently, the temperature was increased from room temperature to 800 °C within 30–45 min. The sample was then annealed for 2 h at these conditions. After annealing, isothermal decompression from P=3 GPa to P=2.7 GPa at 800 °C was performed within a few minutes, followed by static annealing for a period of between 30 min and 18 h. The pressure of 2.7 GPa is about 0.1 GPa below that of the univariant equilibrium coesite–quartz at 800 °C [41,42]. Quenching of the samples after annealing was achieved by switching off the furnace, causing the temperature to drop below 500 °C within a few seconds.

8.2. Quartz microstructures developed in coesite–quartz transformation experiments

The microstructures of the quenched samples were inspected by polarizing microscopy in thin sections oriented normal to the sample axis. The phase assemblage and microstructures were found to be variable even for samples with nominally identical experimental conditions. This variability is attributed to the large uncertainty in pressure inherent in the design of the decompression experiments, which is related to friction in the piston and sample assembly. Notwithstanding, the quenched run products are interpreted to represent various stages of the transformation process and provide the desired insight into fabric evolution related to the progress of the transformation.

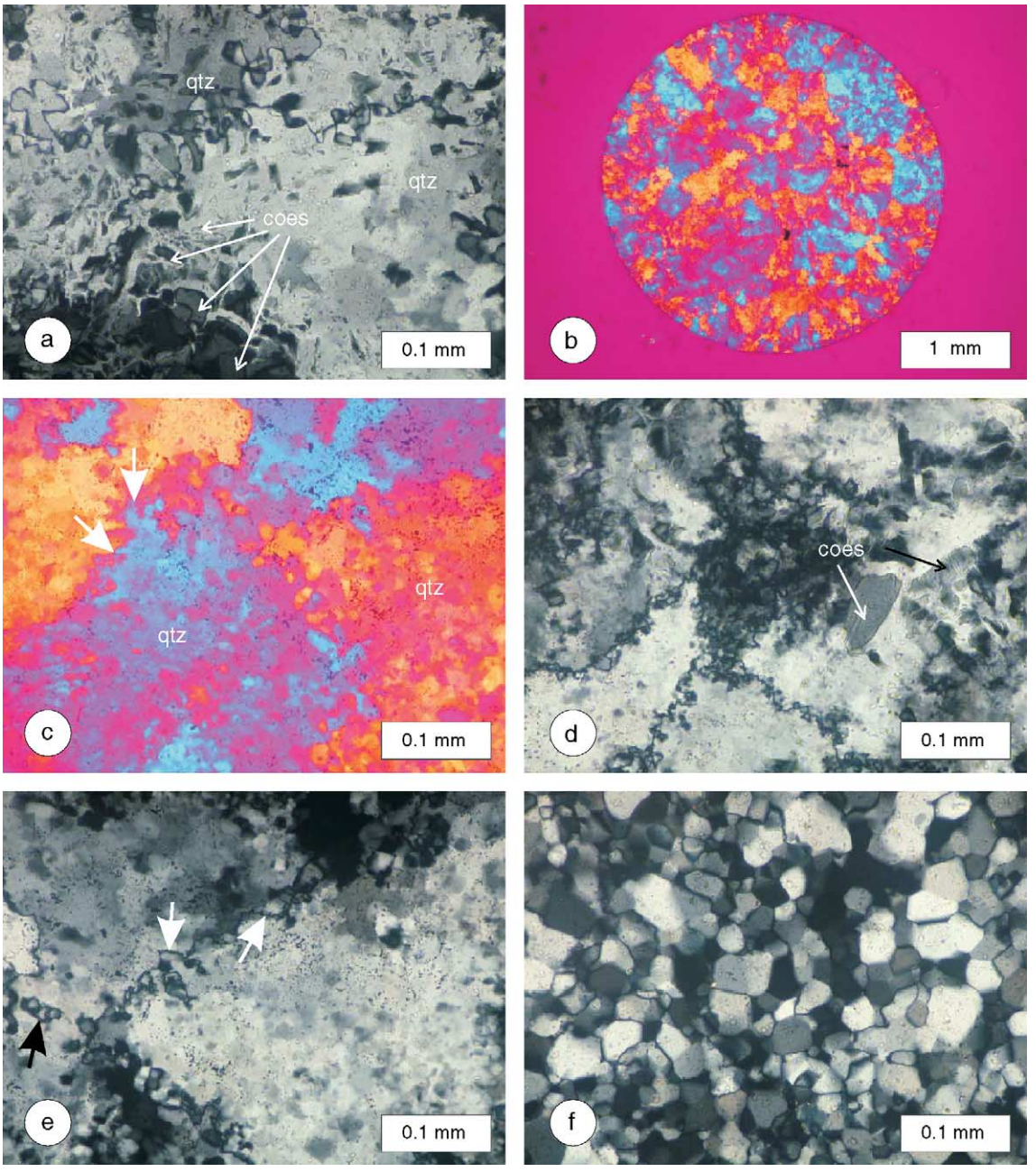

Fig. 12. Optical micrographs (crossed polarizers) showing characteristic microstructures of quartz developed from synthetic coesitite upon isothermal decompression from 3 to 2.7 or 2.0 GPa at 800 °C and subsequent annealing: (a) Poikiloblastic quartz indicating growth along the former high angle grain boundaries of coesite, starting from a few nuclei (sample CW 46, annealed for 17 h at 2.7 GPa). (b) Domains of quartz with similar orientation about 0.3 mm in diameter are thought to represent the volume grown from a single nucleus (sample CW 21, annealed for 2.5 h at 2 GPa). (c) The quartz domains shown in (b) are composed of subgrains with a diameter on the order of 0.01 mm and reveal highly sutured high angle grain boundaries in regions with high misorientation between adjacent domains (sample CW 21, annealed for 2.5 h at 2 GPa). (d) Relic coesite crystals embedded in quartz. A large crystal appears optically strain-free (white arrow), while another one is segmented by crosscutting quartz veinlets (black arrow) (sample CW 21, annealed for 2.5 h at 2 GPa). (e) Quartz domains of similar orientation comprise subgrains with a characteristic diameter on the order of 0.01 mm; the high angle grain boundaries between the domains are extremely sutured (white arrows) with a wavelength of 0.005–0.1 mm (sample CW 21, annealed for 2.5 h at 2 GPa). (f) Foam microstructure of optically strain-free quartz grains with plane or simply curved high angle grain boundaries, indicating grain growth after recovery and recrystallization (sample CW 47, annealed for 18 h at 2.7 GPa).

In most experiments, less than 7% of quartz had formed after annealing for between 30 and 60 min, about 15–30% after 2–6 h, and more than 85% when annealing times exceeded 8 h. Thus, the transformation of the synthetic polycrystalline coesite to quartz proceeds rapidly on laboratory time scales at conditions close to equilibrium. This is in accordance with results obtained by Livshits et al. [43], Mosenfelder and Bohlen [36], and Schönbohm [44].

Samples annealed for up to 2 h show early stages of transformation. The microstructures indicate that quartz has nucleated along the high angle grain boundaries between coesite grains, forming thin seams that expanded along the original grain boundaries of coesite (Fig. 12a). A specific orientation relation between quartz and coesite is not obvious; the original site of nucleation cannot be identified. The thickness of the seams can reach several μm. Frequently, the quartz seams enclosing several coesite grains display a single crystal orientation. In our experiments, such poikiloblastic quartz crystals grew to a diameter of about 0.3 mm, as shown on the optical microphotographs (Fig. 12b). The microstructure implies that the initial nucleation rate of quartz is low compared to the rate of growth.

Samples annealed for more than 2 h show an advanced stage of transformation. Coesite is preserved as relics embedded in quartz, with narrow transformation zones (<1 μm wide) occurring inside the coesite crystals along cracks or twin boundaries, as reported by Langenhorst and Poirier [37]. The microstructure suggests that—with progressive transformation—the original quartz single crystal seams develop into fine-grained aggregates, with a grain size of about 0.01 mm or below (Fig. 12c). The origin of quartz as a poikiloblast starting from one nucleus is readily discernible from the similar orientation of the small quartz grains in domains of about 0.3 mm diameter (Fig. 12c). The microstructure indicates that—upon progressive transformation—the quartz poikiloblasts are deformed by dislocation creep, with recovery and rotation recrystallization. Where poikiloblasts with contrasting orientation impinge upon each other, the high-angle grain boundaries separating both domains are strongly sutured by migration recrystallization, with a typical bulge diameter of about 0.01 mm (Fig. 12d,e).

Samples annealed for 2.5 h after isothermal decompression to 2 GPa (instead of 2.7 GPa used in the other experiments) reveal a nearly complete transformation of coesite to quartz (Fig. 12e), with few undeformed coesite relics preserved. The quartz domains of similar orientation, representing the poikiloblasts described above, are composed of subgrains with a diameter of a few microns, and the high angle grain boundaries are again sutured with a wavelength on the order of 0.01 mm.

In all experimental products, the recrystallized fine-grained quartz aggregates are characterized by a predominantly isometric grain shape with a simple grain boundary configuration, suggesting the onset of static grain growth driven by interfacial free energy (Fig. 12f). This must have happened after significant reduction of stored strain energy by primary recrystallization and recovery. Deformation of quartz by dislocation creep, with dynamic recrystallization and recovery, therefore appears to be restricted to the stage of progressive reaction, and is probably driven by the volume change of about 10% inherent in the coesite to quartz phase transformation, as suggested by, e.g. Livshits [45], and Mosenfelder and Bohlen [36].

9. Discussion and conclusions

Mechanical twinning of jadeite requires a local minimum differential stress of 0.3 GPa [26] for the most favourable orientation of the crystal in the stress field. For twinning to occur in less favourably oriented crystals, differential stresses must be even higher. In jadeite-bearing granitic gneisses of the Sesia Zone, western Alps, Trepmann and Stöckhert [27] found a systematic orientation distribution of jadeite crystals with and without mechanical twins. There, inversion of this orientation distribution allowed to constrain the orientation of the principal stress axes and to estimate the magnitude of differential stress. In contrast, no systematic orientation distribution of jadeite crystals with and without twins is found in the samples from the Dora Maira massif in the present study. This is taken to indicate that in this case the grain scale deformation was not driven by externally imposed tectonic stresses, with an approximately uniform orientation on the sample scale, but by an inhomogeneous stress field created internally.

This interpretation is supported by the random orientation distribution of kyanite crystals with and without kinks or deformation bands. Such an orientation distribution on the scale of a thin section cannot be expected for a rock deformed in an externally imposed stress field.

The conditions of deformation, with high magnitudes of local differential stress, are constrained by the microstructural record of the quartz matrix, in which the kyanite and jadeite crystals are embedded. This quartz matrix reveals optically strain-free grains, about 0.2 mm in diameter, with a foam microstructure. Such microstructures result from grain growth driven by interfacial free energy (e.g. [46]) and are readily destroyed by strain induced grain boundary migration (e.g. [47]), when the material undergoes subsequent deformation by dislocation creep. Thus, the foam structure with strain-free quartz grains implies that the deformation of embedded kyanite and jadeite can hardly originate from a late-stage deformation at low temperatures, but must predate grain growth of quartz. Thus, deformation of jadeite and kyanite must have occurred at UHP metamorphism or early during decompression at still high temperatures. In the annealed quartz fabric, the record of this stage of deformation is erased and not more discernible. On the other hand, twinning and kinking must have taken place after the growth of pyrope at UHP metamorphic conditions, as jadeite and kyanite crystals enclosed in pyrope systematically lack any evidence of twinning or crystal plastic deformation.

Reconstructed *P–T* paths for the UHP metamorphic rocks of the Dora Maira Massif [2,16,17] indicate that the quartz stability field was entered at temperatures of about 700–800 °C during exhumation. Based on laboratory experiments [36,38,43,44] at conditions similar to these natural conditions, where the transformation was observed to go to completion within a few hours, the coesite to quartz transformation is expected to have proceeded quasi instantaneously on geological time scales. Thus, we suspect that the microstructural evolution and the time scales of the coesite quartz transformation in natural UHP metamorphic rocks of the Dora Maira Massif may be similar to those observed in laboratory experiments.

The intense plastic deformation of quartz during the transformation, observed in laboratory experiments, is attributed to the volumetric strain ΔV=+10% inherent in the coesite–quartz transformation, which obviously causes a highly inhomogeneous stress field inside the sample related to the spatial progress of the transformation. Although a steady-state quartz microstructure is clearly not achieved in these experiments, the small recrystallized grain size of quartz of about 0.005–0.01 mm can be taken to indicate plastic deformation of the new-formed quartz at relatively high differential stresses, which may well be on the order of some hundreds of MPa (e.g. [48]).

We propose that a similar process has taken place in the polyphase natural rocks during exhumation, with the transient stresses causing mechanical twinning of jadeite and bending or kinking of kyanite. When the coesite–quartz transformation had gone to completion at high temperatures, grain growth obliterated the earlier microstructures of the quartz matrix, while the deformed jadeite and kyanite crystals preserved the record of the short-term inhomogeneous deformation.

The twinned jadeite crystals demonstrate that the magnitude of the differential stresses exceeded 0.3 GPa in many places [26]. For such levels of differential stress at the inferred temperatures of the coesite–quartz transformation (700–800 °C), experimental flow laws for quartz (e.g. [49]) predict very high strain rates, on the order of 10^{-7} s^{-1} or above. Or, inversely, stresses on the order of hundreds of MPa at temperatures of 700–800 °C can only be attained if loading is fast compared to relaxation, i.e. at strain rates comparable to those typically achieved in laboratory experiments.

As the samples do not show evidence of any significant post-UHP bulk strain on the mesoscopic scale, the stage of high-stress deformation must have been very short-lived and not notably affected by externally imposed tectonic stress. Furthermore, in view of the random orientation distribution of the deformation features in kyanite and jadeite, the orientation of the stress field must have been highly inhomogeneous on the grain scale and controlled by the local progress of the transformation. Notably, the inhomogeneous stress field on the grain scale does not reconcile with an origin of the high stress deformation features by deep faulting, as proposed by e.g. Hwang et al. [15] in their study on eclogites. In combination, the observations suggest that the transformation of coesite to quartz was very rapid, comparable in time scale to the laboratory experi-

ments and that conspicuous deformation features in UHP metamorphic rocks can be attributed to inhomogeneous volumetric straining during phase transformation of major constituents.

Acknowledgements

We thank Hans-Peter Schertl for providing invaluable information on outcrops and petrology of the Brossasco–Isasca Unit, Rolf Neuser for support during SEM work, and Claudia Trepmann for help and advice with the microfabric analysis. An anonymous referee is thanked for the constructive review. Financial support by the Deutsche Forschungsgemeinschaft within the scope of collaborative research center 526 "Rheology of the Earth—From the Upper Crust into the Subduction Zone" (SFB 526) is gratefully acknowledged.

References

[1] B. Stöckhert, Stress and deformation in subduction zones; insight from the record of exhumed metamorphic rocks, Geol. Soc. Spec. Publ. 200 (2002) 255–274.
[2] D. Rubatto, J. Hermann, Exhumation as fast as subduction? Geology (Boulder) 29 (1) (2001) 3–6.
[3] C. Chopin, Ultrahigh-pressure metamorphism; tracing continental crust into the mantle, Earth Planet. Sci. Lett. 212 (1–2) (2003) 1–14.
[4] G.G. Biino, R. Compagnoni, Very-high pressure metamorphism of the Brossasco coronite metagranite, southern Dora Maira Massif, Western Alps, Schweiz. Mineral. Petrogr. Mitt. 72 (1992) 347–363.
[5] S.R. Wallis, A. Ishiwatari, T. Hirajima, K. Ye, J. Guo, D. Nakamura, T. Kato, M. Zhai, M. Enami, B. Cong, S. Banno, Occurrence and field relationships of ultrahigh-pressure metagranitoid and coesite eclogite in the Su-Lu Terrane, eastern China, J. Geol. Soc. (Lond.) 154 (1) (1997) 45–54.
[6] M. Krabbendam, A. Wain, T.B. Andersen, Pre-Caledonian granulite and gabbro enclaves in the Western Gneiss region, Norway; indications of incomplete transition at high pressure, Geol. Mag. 137 (3) (2000) 235–255.
[7] R. Oberhaensli, G. Martinotti, R. Schmid, X. Liu, Preservation of primary volcanic textures in the ultrahigh-pressure terrain of Dabie Shan, Geology (Boulder) 30 (8) (2002) 699–702.
[8] A. Michard, C. Henry, C. Chopin, Structures in UHPM rocks: a case study from the Alps, in: R.C. Coleman, X. Wang (Eds.), Ultrahigh Pressure Metamorphism, University Press, Cambrige, 1995, pp. 132–158.
[9] G.R. Tilton, L. Ames, H.P. Schertl, W. Schreyer, Reconnaissance isotopic investigations on rocks of an undeformed granite contact within the coesite-bearing unit of the Dora Maira Massif, in: W. Schreyer, B. Stoeckhert (Eds.), High Pressure Metamorphism in Nature and Experiment, Lithos, vol. 41, 1–3, 1997, pp. 25–36.
[10] J. Renner, B. Stöckhert, A. Zerbian, K. Roeller, F. Rummel, An experimental study into the rheology of synthetic polycrystalline coesite aggregates, J. Geophys. Res., B 106 (9) (2001) 19411–19429.
[11] A. Lenze, B. Stöckhert, Deformation of metagranitoid rocks of the Dora Maira Massif, Western Alps, during UHP metamorphism or during low grade metamorphic overprint? Beih. Eur. J. Min. 15 (2003) 117.
[12] B. Stöckhert, J. Renner, Rheology of crustal rocks at ultrahigh pressure, in: B.R. Hacker, J.G. Liou (Eds.), When Continents Collide: Geodynamics and Geochemistry of Ultrahigh-Pressure Rocks, Kluwer Academic, Dordrecht, 1998, pp. 57–95.
[13] L.E. Webb, B.R. Hacker, L. Ratschbacher, M. Leech, S. Dong, L. Peng, Mesozoic tectonism in the Qinqing–Dabie collisional orogen; new constraints on the multistage exhumation of ultrahigh-pressure rocks, Geol. Soc. Am. 29 (6) (1997) 119.
[14] Z.Y. Zhao, A.M. Fang, L.J. Yu, High- to ultrahigh-pressure (UHP) ductile shear zones in the Sulu UHP metamorphic belt, China: implications for continental subduction and exhumation, Terra Nova 15 (5) (2003) 322.
[15] S.-L. Hwang, P. Shen, T.-J. Qui, H.-T. Chu, Defect microstructures of minerals as a potential indicator of extremely rapid and episodic exhumation of utrahigh-pressure metamorphic rock: implication to continental collision orogens, Earth Planet. Sci. Lett. 192 (2001) 57–63.
[16] C. Chopin, Coesite and pure pyrope in high-grade blueschists of the Western Alps; a first record and some consequences, Contrib. Mineral. Petrol. 86 (2) (1984) 107–118.
[17] H.-P. Schertl, W. Schreyer, C. Chopin, The pyrope-coesite rocks and their country rocks at Parigi, Dora Maira Massif, Western Alps: detailed petrography, mineral chemistry and *PT*-path, Contrib. Mineral. Petrol. 108 (1991) 1–21.
[18] R. Compagnoni, T. Hirajima, R. Turello, D. Castelli, Ultra high pressure metamorphism in the continental crust, High Pressure Metamorphism in the Western Alps "16th General Meeting of the International Mineralogical Association", 1994.
[19] C. Chopin, H.-P. Schertl, The UHP unit in the Dora-Maira Massif, Western Alps, Int. Book Ser. 4 (2000) 133–148.
[20] D. Gebauer, H.-P. Schertl, M. Brix, W. Schreyer, 35 Ma old ultrahigh-pressure metamorphism and evidence for very rapid exhumation in the Dora Maira Massif, Western Alps, in: W. Schreyer, B. Stöckhert (Eds.), High Pressure Metamorphism in Nature and Experiment, Lithos, vol. 41, 1997, pp. 5–24.
[21] N.H. Schmidt, N. Olesen, Computer-aided determination of crystal-lattice orientation from electron-channeling patterns in the SEM, Can. Mineral. 27 (1989) 15–17.
[22] J. Duyster, Stereo Nett 2.46, University of Bochum, 1997.
[23] C.B. Raleigh, J.L. Talbot, Mechanical twinning in naturally and experimentally deformed diopside, Am. J. Sci. 265 (1967) 151–165.
[24] S.H. Kirby, J.M. Christie, Mechanical twinning in diopside $Ca(Mg,Fe)Si_2O_6$: structural mechanism associated crystal defects, Phys. Chem. Miner. 1 (1977) 137–163.

[25] J.J. Kollé, J.D. Blacic, Deformation of single-crystal clinopyroxenes: 1. Mechanical twinning in diopside and hedenbergite, J. Geophys. Res. 87 (1982) 4019–4034.
[26] J. Orzol, C. Trepmann, B. Stöckhert, G. Shi, Critical shear stress for mechanical twinning of jadeite—an experimental study, Tectonophysics 372 (2003) 135–145.
[27] C. Trepmann, B. Stöckhert, Mechanical twinning of jadeite—an indication of synseismic loading beneath the brittle–plastic transition, Geol. Rundsch. 90 (2001) 4–13.
[28] A. Nicolas, J.P. Poirier, Crystalline Plasticity and Solid State Flow in Metamorphic Rocks, Wiley-Interscience, New York, 1976, 444 pp.
[29] C.J.L. Wilson, J.P. Burg, J.C. Mitchell, The origin of kinks in a polycrystalline ice, Tectonophysics 127 (1986) 27–48.
[30] I. Borg, J. Handin, Experimental deformation of crystalline rocks, Tectonophysics 3 (1966) 249–368.
[31] J.F. Dewey, Nature and origin of kink-bands, Tectonophysics 1 (1965) 459–494.
[32] N.C. Gay, L.E. Weiss, The relationship between principal stress direction and the geometry of kinks in foliated rocks, Tectonophysics 21 (1973) 287–300.
[33] F.A. Donath, Experimental stüdy of kinkband development in Martinsburg slate, in: A.J. Baer, D.K. Norris (Eds.), Research in Tectonics, Geol. Surv. Can. Pap., vol. 68-52, 1968, pp. 255–288.
[34] C.B. Raleigh, Glide mechanisms in experimentally deformed minerals, Science 150 (1965) 739–741.
[35] C. Chopin, C. Henry, A. Michard, Geology and petrology of the coesite-bearing terrain, Dora Maira Massif, Western Alps, Eur. J. Mineral. 3 (1991) 263–291.
[36] J.L. Mosenfelder, S.R. Bohlen, Kinetics of the coesite to quartz transformation, Earth Planet. Sci. Lett. 153 (1997) 133–147.
[37] F. Langenhorst, J.P. Poirier, Transmission electron microscopyof coesite inclusions in the Dora Maira high-pressure metamorphic pyrope-quartzite, Earth Planet. Sci. Lett. 203 (2002) 793–803.
[38] R. Wirth, B. Stöckhert, Transformation of coesite to quartz: microstructures in nature and experiment, in: W. Schreyer, F. Rummel, B. Stöckhert (Eds.), Abstract Volume: Intern. Coll. High Pressure Metamorphism in Nature and Experiment, Bochumer Geologische und Geotechnische Arbeiten, vol. 44, 1995, pp. 260–262.
[39] J. Renner, A. Zerbian, B. Stöckhert, Microstructures of synthetic polycrystalline coesite aggregates–the effect of pressure, temperature, and time, in: W. Schreyer, B. Stöckhert (Eds.), High Pressure Metamorphism in Nature and Experiment, Lithos, 41, 1997, pp. 169–184.
[40] M. Koch-Müller, OH^- in synthetic and natural coesite, Am. Mineral. 88 (2003) 1436–1445.
[41] P.W. Mirwald, H.-J. Massonne, The low-high quartz and quartz–coesite transition to 40 kbar between 600 and 1600 °C and some reconnaissance data on the effect of $NaAlO_2$ component on the low quartz–coesite transition, J. Geophys. Res. 85 (1980) 6983–6990.
[42] S.R. Bohlen, A.L. Boettcher, The quartz–coesite transformation: a precise determination and the effects of other components, J. Geophys. Res. 87 (1982) 7073–7078.
[43] L.D. Livshits, L.V. Larionov, I.S. Delitsin, V.P. Petrov, V.E. Svintitskich, On the possibility of direct coesite–quartz transformation at high pressure, High Temp. High Press. 4 (3) (1972) 311–316.
[44] D. Schönbohm, Untersuchung zur Kinetik der Coesit—Quarz Umwandlung unter in-situ Bedingungen mittels Synchrotronstrahlung sowie Analyse der Mikrostrukturen im Transformationsbereich mittels TEM, Dissertation, Bonn, 2003, 135 pp.
[45] L.D. Livshits, Polymorphic transformation of coesite into quartz at high confining pressures, Phys. Solid Earth 19 (7) (1983) 554–556.
[46] B. Evans, J. Renner, G. Hirth, A few remarks on the kinetics of static grain growth in rocks, Int. J. Earth Sci. 90 (1) (2001) 88–103.
[47] J.L. Urai, W.D. Means, G.S. Lister, Dynamic recrystallization of minerals, Geophys. Monogr. 36 (1986) 161–199.
[48] R. Twiss, Theory and applicability of a recrystallized grain size paleopiezometer, Pure Appl. Geophys. 115 (1–2) (1977) 227–244.
[49] M.S. Paterson, F.C. Luan, Quartzite rheology under geological conditions, Geol. Soc. Spec. Publ. 54 (1990) 299–307.
[50] C. Henry, Ĺunité à coesite du massif Dora-Maira dans son cadre pétrologique et structural (Alpes occidentales, Italie), unpublished Doctoral thesis, University of Paris, France, 1993, p. 284.
[51] G. Simon, C. Chopin, V. Schenk, Near-end-member magnesiochloritoid in prograde-zoned pyrope, Dora-Maira Massif, Western Alps, Lithos 41 (1–3) (1997) 37–57.
[52] N.L. Carter, C.B. Raleigh, Principal stress directions from plastic flow in crystals, Geol. Soc. Amer. Bull. 80 (1969) 1231–1264.